Advances in Nano Research, *Vol. 17, No.2 (2024) 95-107*
https://doi.org/10.12989/anr.2024.17.2.095

Nonlinear dynamic stability and vibration analysis of sandwich FG-CNTRC shallow spherical shell

Kamran Foroutan[1a], Akin Atas[2b] and Habib Ahmadi*[1]

[1]*Faculty of Mechanical Engineering, Shahrood University of Technology, Shahrood, Iran*
[2]*Department of Mechanical, Aerospace and Civil Engineering, University of Manchester, UK*

(*Received March 20, 2021, Revised October 18, 2022, Accepted July 29, 2024*)

Abstract. In this article, the semi-analytical method was used to analyze the nonlinear dynamic stability and vibration analysis of sandwich shallow spherical shells (SSSS). The SSSS was considered as functionally graded carbon nanotube-reinforced composites (FG-CNTRC) with three new patterns of FG-CNTRC. The governing equation was obtained and discretized utilizing the Galerkin method by implementing the von Kármán-Donnell nonlinear strain-displacement relations. The nonlinear dynamic stability was analyzed by means of the fourth-order Runge-Kutta method. Then the Budiansky-Roth criterion was employed to obtain the critical load for the dynamic post-buckling. The approximate solution for the deflection was represented by suitable mode functions, which consisted of the three modes of transverse nonlinear oscillations, including one symmetrically and two asymmetrical mode shapes. The influences of various geometrical characteristics and material parameters were studied on the nonlinear dynamic stability and vibration response. The results showed that the order of layers had a significant influence on the amplitude of vibration and critical dynamic buckling load.

Keywords: dynamic post-buckling; FG-CNT material; sandwich shallow spherical shells (SSSS); vibration analysis

1. Introduction

The spherical shells with advanced materials have great application potential in several engineering structures and industrial applications, including aircraft and aerospace engineering. For example, spherical shells are widely used in many structures, such as missiles, radar warheads, and submarines. Also, the spherical geometry is assumed as an ideal structure for the pressure hulls of deep submersibles (Pan and Cui 2010, 2011). In this regard, carbon nanotubes (CNTs), one of the advanced materials with extraordinary stiffness and tensile strength, are used as reinforcing components for composite spherical shells. Depending on the application type, these shell structures may be exposed to different types of static and dynamic loads. Recently, the research on analyzing the structures with these materials has been the scientists' interest (Lei *et al.* 2015, Zhu *et al.* 2012, Wang *et al.* 2011, Phung-Van *et al.* 2018). Therefore, the stability and dynamic analysis of these structures under different loads are very important.

Some researchers have concentrated on the field of static buckling analysis of the shell structures subjected to mechanical and thermal loading with various theories (Huang 1964, Tillman 1970, Wunderlich and Albertin 2002, Wang *et al.* 2019, Shahsiah *et al.* 2011, Bich and Van Tung 2011, Anh *et al.* 2015). Huang (1964) studied the axi-symmetrical buckling analysis of the clamped shallow shells with spherical shape subjected to external excitation regarding unsymmetrical deflection condition. Tillman (1970) presented a theoretical and experimental study for the buckling analysis of elastic clamped shallow spherical caps, which were uniformly subjected to external pressure. The buckling analysis of an imperfect spherical shallow shell was addressed by Wunderlich and Albertin (2002). Wang *et al.* (2019) established the general similitude requirements and the scaling laws for nonlinear buckling of stiffened orthotropic shallow spherical shells utilizing the energy approach. Shahsiah *et al.* (2011) addressed the thermal instability of deep shells with a spherical shape made of FG material. In this study, regarding the Sanders nonlinear kinematics equations and utilizing the first-order shear deformation theory (FSDT) of shells, the nonlinear partial equations of motion were extracted. Bich and Van Tung (2011) investigated the axisymmetric nonlinear response of FG shallow shells via an analytical method. In this work, the spherical shell was uniformly exposed to external pressure, including the temperature effects, and also the Bubnov-Galerkin and Runge-Kutta methods are utilized to discretize and solve these equations, respectively. The nonlinear stability analysis of thin FG and eccentrically stiffened FG annular spherical shells resting on elastic foundations under external pressure and thermal loads was investigated (Anh *et al.* 2015, Duc *et al.* 2016).

Some researchers have focused on the dynamic buckling and vibration behavior of the shell and plate structures. The dynamic response behavior of a shallow spherical shell and laminated anisotropic spherical caps with a clamped edge under uniform load was investigated by Ganapathi and Varadan (1982, 1995). Ye (1997) investigated the dynamic

*Corresponding author, Ph.D.,
E-mail: habibahmadif@shahroodut.ac.ir
[a] Ph.D., E-mail: kamran.foroutan@shahroodut.ac.ir
[b] Ph.D., E-mail: akin.atas@manchester.ac.uk

ISSN: 2287-237X (Print), 2287-2388 (Online)

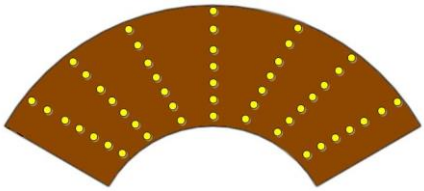

(a) UD

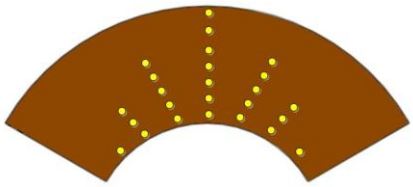

(b) FG-Λ

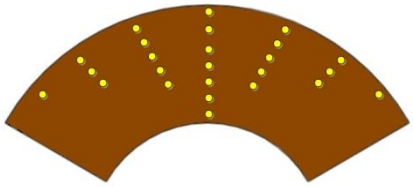

(c) FG-V

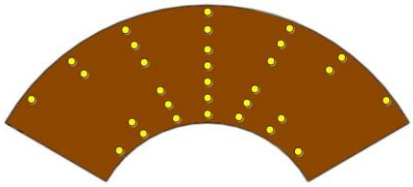

(d) FG-X

Fig. 1 Configuration of the four sub-patterns of CNT distribution for cylindrical panel

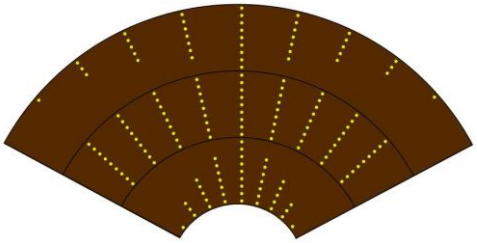

(a) Type1: FG V-UD-FG Λ

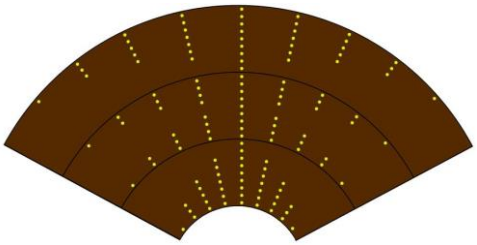

(b) Type2: FG V-X-Λ

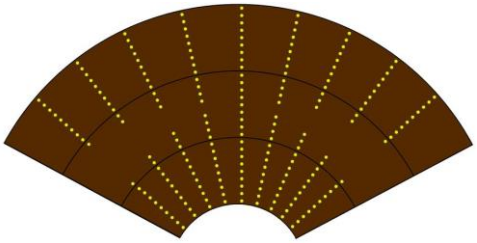

(c) Type3: UD-FG X-UD

Fig. 2 The sandwich shallow spherical shells with three types of layers of FG-CNTRC

instability and nonlinear vibration of thin shallow shells with two spherical and conical shapes, which were under in-plane and periodic transverse loads. In this study, using the dynamic equations of the Marguerre type and the Galerkin approach, the behaviors of shallow shells were analyzed. Prakash *et al.* (2007) utilized an axisymmetric analysis to investigate the dynamic buckling of spherical caps with FG material in a thermal environment subjected to pressure load. In this study, considering the nonlinear von Kármán equation and the FSDT, governing equations were derived. Also, the nonlinear equations of motion were solved by applying the technique of Newmark's integration regarding the modified Newton–Raphson iteration scheme. Duc (2018) investigated the nonlinear dynamic response of higher- order shear deformable sandwich FG circular cylindrical shells with outer surface-bonded piezoelectric actuator on elastic foundations subjected to thermo-electro-mechanical and damping loads. The vibration and nonlinear dynamic behaviors of the shear deformable plates resting on elastic foundations was investigated by Dat *et al.* (2022). In (Duc 2013, Quan and Duc 2016, Duc *et al.* 2017a), the nonlinear dynamic and vibration behavior of the stiffened FG shallow shells, FG double-curved shallow shells, and S-FG shallow spherical shells subjected to mechanical and thermal loading were studied. In these works, the shells with or without elastic foundations as Pasternak type and initial imperfection were investigated.

Despite their extensive usage in a diversity of industrial applications like pressure vessel, submarine hulls and etc., the buckling and vibration analysis of the FG-CNTRC structures were not addressed in the previously mentioned-work. The vibration and nonlinear dynamic behaviors of the sandwich FG-CNTRC plate with a porous core layer was investigated by Thanh *et al.* (2017). The vibration behavior of the FG-CNTRC shallow shells with various boundary conditions subjected to mechanical or thermal loading was investigated (Wang *et al.* 2017, Duc *et al.* 2019, Wang *et al.* 2018, Thomas and Roy 2016). Manh *et al.* (2020) presented the nonlinear post-buckling behavior of carbon nanotubes reinforced sandwich composite annular spherical shells resting on elastic foundations in the thermal environment. The nonlinear dynamic response and vibration behavior of the FG-CNTRC nanocomposite elliptical cylindrical shells resting on elastic foundations were analyzed by Dat *et al.* (2020). Nonlinear buckling and post-buckling of FG-CNTRC truncated conical shells, and thermal and mechanical stability of FG-CNTRC truncated conical shells resting on elastic foundations were investigated (Duc *et al.* 2017b, Chan *et al.* 2019). Recently, the dynamic buckling analyses of FG-CNTRC cylindrical shell under axial power-law time-varying displacement load were investigated by Jiao *et al.* (2019). In this study, employing the FSDT and nonlinear von Kármán relationships, the governing equations for the dynamic buckling behavior of FG-CNTRC cylindrical shell with thermal effects were derived. Also, the nonlinear dynamic thermal buckling of sandwich

spherical and conical shells with CNT reinforced face-sheets was addressed by Sankar *et al.* (2017). Also, recently, some researchers have investigated various analyses of the FG-CNTRC structures (Asadi and Wang 2017, Cong *et al.* 2022, Fu *et al.* 2021, Foroutan *et al.* 2021). Asadi and Wang (2017) presented the dynamic stability analysis of a pressurized FG-CNTRC cylindrical shell interacting with supersonic airflow. Cong *et al.* (2022) studied the vibration and nonlinear dynamic response of temperature-dependent FG-CNTRC laminated double-curved shallow shell with positive and negative Poisson's ratios. Fu *et al.* (2021) examined the dynamic instability analysis of FG-CNTRC laminated conical shells resting on elastic foundations. Foroutan *et al.* (2021a) investigated the static and dynamic hygrothermal post-buckling analysis of sandwich cylindrical panels with an FG-CNTRC core embedded within nonlinear viscoelastic foundations. It should be explained that the geometry and analysis of the above-mentioned research are different from the present study. So that, in this study the nonlinear dynamic stability and vibration analysis of sandwich FGCNTRC shallow spherical shell is investigated. Furthermore, in this study, the sandwich shallow spherical shell with three new patterns of FG-CNTRC consisting of FG V-UD- FG Λ, FG V-X-Λ, and UD-FG X-UD have been constructed.

To the best of the authors' knowledge, the nonlinear dynamic stability and vibration of sandwich functionally graded carbon nanotube-reinforced composite (FG-CNTRC) shallow spherical shells have not been investigated. In this study, sandwich FG-CNTRC shallow spherical shells with three new patterns of FG-CNTRC are investigated for the first time using the semi-analytical method. Two kinds of CNTRC shells, namely, uniformly distributed (UD) and functionally graded (FG) reinforcements, are assumed. In this context, four sub-patterns of CNT distribution have been considered, that is, FG-X, FG-Λ, FG-V, and UD (see Fig. 1) (Ebrahimi and Habibi 2017, Jamali *et al.* 2019, Foroutan *et al.* 2019, 2021a, Tayeb *et al.* 2020, Hashemi *et al.* 2021). The CNTs are uniformly distributed along the thickness direction, which is named the UD (Fig. 1a). For the FG-Λ case, the outer surface is free of the CNTs, and the inner surface is CNT-rich, whereas, for the FG-V case, the reverse pattern is considered (see Figs. 1b and c). In the FG-X case, the outer and the inner surfaces are CNT-rich (see Fig. 1d). So, the novelties of the present paper are as follows: Using these sub-patterns, the sandwich shallow spherical shell with three new patterns of FG-CNTRC have been constructed consisting of FG V-UD- FG Λ, FG V-X-Λ, and UD-FG X-UD (see Fig 2). In principle, in this study, the sandwich shallow spherical shell with three layers is considered that one of the four sub-patterns of CNT is distributed in each layer, and consequently, three new patterns, which are considered in this study, are created. In the FG V-UD-FG Λ and FG V-X-Λ cases, the upper layer is FG V, the lower layer is FG Λ, and the middle layer is UD and FG X, respectively (see Figs. 2a and b). Also, for the UD-FG X-UD case, the upper and lower layer is UD, and the middle layer is FG X (see Fig. 2c). The governing equations are obtained and analyzed utilizing the theory of classical shell, nonlinear von Kármán- Donnell relations, Galerkin method, Runge-Kutta approach, and the Budiansky-Roth criterion. The approximate solution for the deflection is represented by suitable mode functions, which consist of the three modes of transverse nonlinear oscillations, including one symmetrically deformed shape and two asymmetrical mode shapes. Results are examined to investigate the effects of geometrical characteristics, initial imperfection, and material properties on the nonlinear dynamic stability and vibration analysis of the sandwich FG-CNTRC shallow spherical shells.

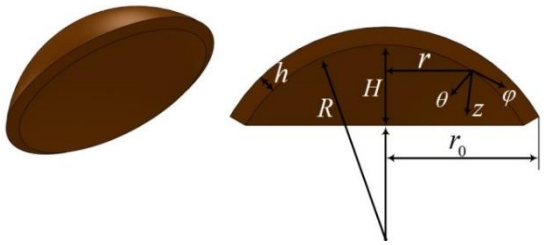

Fig. 3 The sandwich FG-CNTRC shallow spherical shells

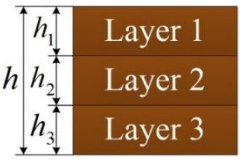

Fig. 4 The layers of the sandwich FG-CNTRC shallow spherical shells

2. Sandwich FG-CNTRC shallow spherical shells

Fig. 3 illustrates the sandwich FG-CNTRC shallow spherical shells with thickness h, the radius of curvature R, and base radius r_0 in the (φ, θ, z) coordinate system. θ, φ, and z show the circumferential, meridional, and radial-thickness directions. In addition, the three layers of the shell are shown in Fig. 4, where h_1, h_2, and h_3 are the thickness of layers 1, 2, and 3, respectively.

The shear modulus, effective mass density, and Young's modulus of CNTRCs are calculated based on Eq. (1) (Ebrahimi and Habibi 2017, Jamali *et al.* 2019, Foroutan *et al.* 2019, 2021a, b):

$$\begin{aligned} G_{12} &= \eta_3 \left(\frac{G_{12}^{CNT} G^m}{V_{CNT} G^m + V_m G_{12}^{CNT}} \right), \\ \rho &= V_{CNT} \rho^{CNT} + V_m \rho^m \\ E_{11} &= \eta_1 V_{CNT} E_{11}^{CNT} + V_m E^m, \\ E_{22} &= \eta_2 \left(\frac{E_{22}^{CNT} E^m}{V_{CNT} E^m + V_m E_{22}^{CNT}} \right) \end{aligned} \tag{1}$$

V_m and V_{CNT} are volume fractions of the matrix and the CNT, respectively, which are satisfied by the relation $V_m + V_{CNT} = 1$. The load transferred between the polymeric phase, and the CNT is less than perfect; therefore, $\eta_i (i = 1,2,3)$ (the parameter of the CNT efficiency) is used to consider the small-scale influence and other effects on properties of the CNTRCs material, which is presented in Eq. (1) (Thai *et al.* 2018). In this work, the estimation of $\eta_i (i = 1,2,3)$ according to the E_{11}, E_{22}, and G_{12} of

CNTRCs is predicted from the extended mixture rule to those from the molecular dynamics simulations given by Shen (Shen and Zhang 2010, Shen and Zhu 2010), and the values of them are listed in Table 4. It is assumed that the CNTRC layer is made of single-wall carbon nanotubes (SWCNT) and isotropic matrix. The CNT is distributed along the thickness direction for the shell layers as UD or FG (Foroutan *et al.* 2019, Seidel and Lagoudas 2006).

According to Fig. 1, the relation of CNT volume fractions (V_{CNT}) for four types of FG-CNTRC shells (Fig. 1), which represents the density of CNTs in the matrix, are as follows (Tounsi *et al.* 2013, Aydogdu 2014, Ebrahimi and Habibi 2017, Jamali *et al.* 2019, Foroutan *et al.* 2019, 2021a, Tayeb *et al.* 2020, Hashemi *et al.* 2021, Khadimallah *et al.* 2021):

$$V_{CNT}(z)=\begin{cases} V_{CNT}^{*} & \text{(UD CNTRC)}\\ 2V_{CNT}^{*}\left(1-\dfrac{2z}{h}\right) & \text{(FG}-\text{V CNTRC)}\\ V_{CNT}^{*}\left(1+\dfrac{2z}{h}\right) & \text{(FG}-\Lambda\text{ CNTRC)}\\ 4V_{CNT}^{*}\left(\dfrac{|z|}{h}\right) & \text{(FG}-\text{X CNTRC)}\end{cases} \tag{2}$$

Considering Figs. 2 and 4 and Eq. (2), we have suggested a three-layer shell so that each layer has sub-patterns of CNT distribution. Then, using Eq. (2) and applying the continuity condition, the CNTs volume fraction relation for the sandwich shell with three CNTs distribution patterns can be written as follows:

Type 1: FG V-UD-FG Λ

$$V_{CNT}(z)=\begin{cases} \text{FG}-V\text{:}\quad 2V_{CNT}^{*}\left(1-\dfrac{2z}{h}\right) & -\dfrac{h}{2}\le z\le -\dfrac{h}{2}+h_1\\ \text{UD:}\quad V_{CNT}^{*} & -\dfrac{h}{2}+h_1\le z\le \dfrac{h}{2}-h_3\\ \text{FG}-\Lambda\text{:}\ V_{CNT}^{*}\left(1+\dfrac{2z}{h}\right) & \dfrac{h}{2}-h_3\le z\le \dfrac{h}{2}\end{cases} \tag{3a}$$

Type 2: FG V-X-Λ

$$V_{CNT}(z)=\begin{cases} \text{FG}-V\text{:}\quad 2V_{CNT}^{*}\left(1-\dfrac{2z}{h}\right) & -\dfrac{h}{2}\le z\le -\dfrac{h}{2}+h_1\\ \text{FG}-X\text{:}\ 4V_{CNT}^{*}\left(\dfrac{|z|}{h}\right) & -\dfrac{h}{2}+h_1\le z\le \dfrac{h}{2}-h_3\\ \text{FG}-\Lambda\text{:}\ V_{CNT}^{*}\left(1+\dfrac{2z}{h}\right) & \dfrac{h}{2}-h_3\le z\le \dfrac{h}{2}\end{cases} \tag{3b}$$

Type 3: UD-FG X-UD

$$V_{CNT}(z)=\begin{cases} \text{UD:}\quad V_{CNT}^{*} & -\dfrac{h}{2}\le z\le -\dfrac{h}{2}+h_1\\ \text{FG}-X\text{:}\ 4V_{CNT}^{*}\left(\dfrac{|z|}{h}\right) & -\dfrac{h}{2}+h_1\le z\le \dfrac{h}{2}-h_3\\ \text{UD:}\quad V_{CNT}^{*} & \dfrac{h}{2}-h_3\le z\le \dfrac{h}{2}\end{cases} \tag{3c}$$

where

$$V_{CNT}^{*}=\frac{w_{CNT}}{w_{CNT}+\left(\frac{\rho_{CNT}}{\rho_m}\right)-\left(\frac{\rho_{CNT}}{\rho_m}\right)w_{CNT}} \tag{4}$$

3. Governing equations

The classical shell theory is used to obtain the compatibility and equilibrium equations, and to examine the static and dynamic post-buckling responses. In this study, a new variable is introduced (r), which is defined as $r=R\sin\varphi$. Due to the shallowness of the sandwich spherical shell, it is assumed that $\cos\varphi=1$ and $Rd\varphi=dr$. The strains at z-distance related to mid-plane along the thickness of the spherical shell are as follows:

$$\varepsilon_r=\varepsilon_r^0-z\chi_r;\ \varepsilon_\theta=\varepsilon_\theta^0-z\chi_\theta;\ \gamma_{r\theta}=\gamma_{r\theta}^0-2z\chi_{r\theta} \tag{5}$$

Based on the von Kármán-Donnell nonlinear strain-displacement relations, the components of the strain at the middle surface of the spherical shell are in the following form (Bich and Van Dung 2012):

$$\begin{aligned}\varepsilon_r^0&=\frac{\partial u}{\partial r}-\frac{w}{R}+\frac{1}{2}\left(\frac{\partial w}{\partial r}\right)^2,\\ \varepsilon_\theta^0&=\frac{1}{r}\frac{\partial v}{\partial\theta}+\frac{u}{R}-\frac{w}{R}+\frac{1}{2r^2}\left(\frac{\partial w}{\partial\theta}\right)^2\\ \gamma_{r\theta}^0&=\frac{\partial v}{\partial r}+\frac{1}{r}\frac{\partial u}{\partial\theta}-\frac{v}{r}+\frac{1}{r}\frac{\partial w}{\partial r}\frac{\partial w}{\partial\theta},\qquad \chi_r=\frac{\partial^2 w}{\partial r^2},\\ \chi_\theta&=\frac{1}{r}\frac{\partial w}{\partial r}+\frac{1}{r^2}\frac{\partial^2 w}{\partial\theta^2},\qquad \chi_{r\theta}=\frac{1}{r}\frac{\partial^2 w}{\partial\theta\partial r}-\frac{1}{r^2}\frac{\partial w}{\partial\theta}\end{aligned} \tag{6}$$

where ε_r^0, ε_θ^0, and $\gamma_{r\theta}^0$ are the normal strains and the shear strain at the middle surface of the shell, respectively. Also, χ_r, χ_θ, and $\chi_{r\theta}$ are the twist and curvature changes, respectively.

The compatibility equation of the imperfect spherical shell according to Eqs. (5) and (6), can be expressed as follows:

$$\begin{aligned}&\frac{1}{r^2}\frac{\partial^2\varepsilon_r^0}{\partial\theta^2}-\frac{1}{r}\frac{\partial\varepsilon_r^0}{\partial r}+\frac{1}{r^2}\left(2r\frac{\partial\varepsilon_\theta^0}{\partial r}+r^2\frac{\partial^2\varepsilon_\theta^0}{\partial r^2}\right)\\ &-\frac{1}{r^2}\left(\frac{\partial\gamma_{r\theta}^0}{\partial\theta}+r\frac{\partial^2\gamma_{r\theta}^0}{\partial r\partial\theta}\right)\\ &=-\frac{1}{R}\left(\frac{\partial^2 w}{\partial r^2}+\frac{1}{r}\frac{\partial w}{\partial r}+\frac{1}{r^2}\frac{\partial^2 w}{\partial\theta^2}\right)-\frac{1}{r}\frac{\partial w}{\partial r}\frac{\partial^2 w}{\partial r^2}\\ &-\frac{1}{r^2}\left(\frac{\partial^2 w}{\partial r^2}\frac{\partial^2 w}{\partial\theta^2}-\left(\frac{\partial^2 w}{\partial r\partial\theta}\right)^2\right)\\ &-\frac{2}{r^3}\frac{\partial w}{\partial\theta}\frac{\partial^2 w}{\partial r\partial\theta}-\frac{1}{r^4}\left(\frac{\partial w}{\partial\theta}\right)^2\end{aligned} \tag{7}$$

Based on Hooke's law, the stress-strain relations of sandwich FG-CNTRC shallow spherical shells can be written as (Loy *et al.* 1999):

$$\begin{bmatrix}\sigma_r\\ \sigma_\theta\\ \sigma_{r\theta}\end{bmatrix}=\begin{bmatrix}Q_{11} & Q_{12} & 0\\ Q_{12} & Q_{22} & 0\\ 0 & 0 & Q_{66}\end{bmatrix}\begin{Bmatrix}\varepsilon_r\\ \varepsilon_\theta\\ \gamma_{r\theta}\end{Bmatrix} \tag{8}$$

where

$$\begin{aligned}&Q_{11}=\frac{E_{11}}{1-\nu_{12}\nu_{21}};\ Q_{22}=\frac{E_{22}}{1-\nu_{12}\nu_{21}};\\ &Q_{12}=\frac{\nu_{21}E_{11}}{1-\nu_{12}\nu_{21}};\ Q_{66}=G_{12};\ \nu_{21}=\frac{E_{22}}{E_{11}}\nu_{12}\end{aligned} \tag{9}$$

In Eq. (9), ν_{21} and ν_{12} are Poisson's ratios. σ_r, σ_θ and $\sigma_{r\theta}$ are the normal stresses in radial and tangential directions and the shear stress of the sandwich FG-CNTRC shallow spherical shells, respectively.

To obtain the resultant forces $(N_r, N_\theta, N_{r\theta})$ for the sandwich FG-CNTRC shallow spherical shell, Eq. (8) is integrated over the thickness. The resultant moments $(M_r, M_\theta, M_{r\theta})$ obtain by first multiplying the Eq. (8) by the thickness z and integrating over the thickness. Substituting Eq. (8) into Eqs. (5) and (6), the resultant moments and forces are obtained as follows:

Resultant forces:

$$\begin{aligned} N_r &= A_{11}\varepsilon_r^0 + A_{12}\varepsilon_\theta^0 - B_{11}\chi_r - B_{12}\chi_\theta \\ N_\theta &= A_{12}\varepsilon_r^0 + A_{22}\varepsilon_\theta^0 - B_{12}\chi_r - B_{22}\chi_\theta \\ N_{r\theta} &= A_{66}\gamma_{r\theta}^0 + B_{66}\chi_{r\theta} \end{aligned} \tag{10}$$

Resultant moments:

$$\begin{aligned} M_r &= B_{11}\varepsilon_r^0 + B_{12}\varepsilon_\theta^0 - D_{11}\chi_r - D_{12}\chi_\theta \\ M_\theta &= B_{12}\varepsilon_r^0 + B_{22}\varepsilon_\theta^0 - D_{12}\chi_r - D_{22}\chi_\theta \\ M_{r\theta} &= B_{66}\gamma_{r\theta}^0 + D_{66}\chi_{r\theta} \end{aligned} \tag{11}$$

where the coefficients in Eqs. (10) and (11) are as follows:

$$\begin{aligned} (A_{11}, A_{22}, A_{12}, A_{66}) &= \int_{-\frac{h}{2}}^{\frac{h}{2}} (Q_{11}, Q_{22}, Q_{12}, Q_{66})\,dz \\ (B_{11}, B_{22}, B_{12}, B_{66}) &= \int_{-\frac{h}{2}}^{\frac{h}{2}} (Q_{11}, Q_{22}, Q_{12}, 2Q_{66})\,z\,dz \\ (D_{11}, D_{22}, D_{12}, D_{66}) &= \int_{-\frac{h}{2}}^{\frac{h}{2}} (Q_{11}, Q_{22}, Q_{12}, 2Q_{66})\,z^2\,dz \end{aligned} \tag{12}$$

Considering the classical shell theory, the nonlinear motion equations of the shallow spherical shell are in the following form (Bich and Van Dung 2012, Duc 2014, Duc *et al*. 2017a). Also, in these equations, it is assumed that $u \ll w$ and $v \ll w$ and consequently $\rho_1 \frac{\partial^2 u}{\partial t^2} \to 0$ and $\rho_1 \frac{\partial^2 v}{\partial t^2} \to 0$.

$$\frac{\partial N_r}{\partial r} + \frac{1}{r}\frac{\partial N_{r\theta}}{\partial \theta} + \frac{N_r - N_\theta}{r} = 0 \tag{13}$$

$$\frac{\partial N_{r\theta}}{\partial r} + \frac{1}{r}\frac{\partial N_\theta}{\partial \theta} + \frac{2N_{r\theta}}{r} = 0 \tag{14}$$

$$\begin{aligned} &\frac{1}{r}\left[\frac{\partial^2}{\partial r^2}(rM_r) + 2\left(\frac{\partial^2 M_{r\theta}}{\partial r \partial \theta} + \frac{1}{r}\frac{\partial M_{r\theta}}{\partial \theta}\right) + \frac{1}{r}\frac{\partial^2 M_\theta}{\partial \theta^2} - \frac{\partial M_\theta}{\partial r}\right] \\ &+ \frac{1}{r}\frac{\partial}{\partial r}\left(rN_r\frac{\partial w}{\partial r} + N_{r\theta}\frac{\partial w}{\partial \theta}\right) + \frac{N_r + N_\theta}{R} \\ &+ \frac{1}{r}\frac{\partial}{\partial \theta}\left(N_{r\theta}\frac{\partial w}{\partial r} + \frac{1}{r}N_\theta\frac{\partial w}{\partial \theta}\right) + q = 2\rho_1\mu\frac{\partial w}{\partial t} + \rho_1\frac{\partial^2 w}{\partial t^2} \end{aligned} \tag{15}$$

where q is the external pressure. t is the time, and ρ_1 is obtained in the following form:

$$\rho_1 = \int_{-\frac{h}{2}}^{\frac{h}{2}} \rho\,dz \tag{16}$$

The stress function (ψ) is considered in the following form, which is satisfied by Eqs. (13) and (14):

$$\begin{aligned} N_r &= \frac{1}{r}\frac{\partial^2 \psi}{\partial r^2} + \frac{1}{r^2}\frac{\partial^2 \psi}{\partial \theta^2};\quad N_\theta = \frac{\partial^2 \psi}{\partial r^2}; \\ N_{r\theta} &= \frac{1}{r^2}\frac{\partial \psi}{\partial \theta} - \frac{1}{r}\frac{\partial^2 \psi}{\partial r \partial \theta} \end{aligned} \tag{17}$$

According to Eqs. (10) and (17), one can solve these equations to find ε_r^0, ε_θ^0, and $\gamma_{r\theta}^0$ in terms of N_r, N_θ, and $N_{r\theta}$ as follows:

$$\begin{aligned} \varepsilon_r^0 &= \left(\frac{1}{r}\frac{\partial \psi}{\partial r} + \frac{1}{r^2}\frac{\partial^2 \psi}{\partial \theta^2}\right)d_1 + \frac{\partial^2 \psi}{\partial r^2}d_2 \\ &- \frac{\partial^2 w}{\partial r^2}d_3 - \left(\frac{1}{r}\frac{\partial w}{\partial r} + \frac{1}{r^2}\frac{\partial^2 w}{\partial \theta^2}\right)d_4 \end{aligned} \tag{18a}$$

$$\begin{aligned} \varepsilon_\theta^0 &= \frac{\partial^2 \psi}{\partial r^2}d_5 + \left(\frac{1}{r}\frac{\partial \psi}{\partial r} + \frac{1}{r^2}\frac{\partial^2 \psi}{\partial \theta^2}\right)d_2 \\ &- \left(\frac{1}{r}\frac{\partial w}{\partial r} + \frac{1}{r^2}\frac{\partial^2 w}{\partial \theta^2}\right)d_6 - \frac{\partial^2 w}{\partial r^2}d_7 \end{aligned} \tag{18b}$$

$$\gamma_{r\theta}^0 = \left(\frac{1}{r^2}\frac{\partial \psi}{\partial \theta} - \frac{1}{r}\frac{\partial^2 \psi}{\partial r \partial \theta}\right)d_8 + \left(\frac{1}{r^2}\frac{\partial w}{\partial \theta} - \frac{1}{r}\frac{\partial^2 w}{\partial r \partial \theta}\right)d_9 \tag{18c}$$

where d_i $(i = 1, 2, \ldots, 9)$ are as follows:

$$\begin{aligned} &d_1 = \frac{A_{22}}{\delta};\quad d_2 = -\frac{A_{12}}{\delta}; \\ &d_3 = \frac{(A_{12}B_{12} - A_{22}B_{11})}{\delta};\quad d_4 = \frac{(B_{22}A_{12} - A_{22}B_{12})}{\delta} \\ &d_5 = \frac{A_{11}}{\delta};\quad d_6 = \frac{(A_{12}B_{12} - A_{11}B_{22})}{\delta}; \\ &d_7 = \frac{(B_{11}A_{12} - A_{11}B_{12})}{\delta}\,d_8 = \frac{1}{A_{66}}; \\ &d_9 = -\frac{B_{66}}{A_{66}};\quad \delta = A_{11}A_{22} - A_{12}^2 \end{aligned} \tag{19}$$

To obtain the resultant moments in terms of the resultant forces, Eq. (18) substitutes into Eq. (11) as follows:

$$\begin{aligned} M_r &= \left(\frac{1}{r}\frac{\partial \psi}{\partial r} + \frac{1}{r^2}\frac{\partial^2 \psi}{\partial \theta^2}\right)g_1 + \frac{\partial^2 \psi}{\partial r^2}g_2 \\ &- \frac{\partial^2 w}{\partial r^2}g_3 - \left(\frac{1}{r}\frac{\partial w}{\partial r} + \frac{1}{r^2}\frac{\partial^2 w}{\partial \theta^2}\right)g_4 \end{aligned} \tag{20a}$$

$$\begin{aligned} M_\theta &= \frac{\partial^2 \psi}{\partial r^2}g_5 + \left(\frac{1}{r}\frac{\partial \psi}{\partial r} + \frac{1}{r^2}\frac{\partial^2 \psi}{\partial \theta^2}\right)g_6 \\ &- \left(\frac{1}{r}\frac{\partial w}{\partial r} + \frac{1}{r^2}\frac{\partial^2 w}{\partial \theta^2}\right)g_7 - \frac{\partial^2 w}{\partial r^2}g_8 \end{aligned} \tag{20b}$$

$$M_{r\theta} = \left(\frac{1}{r^2}\frac{\partial \psi}{\partial \theta} - \frac{1}{r}\frac{\partial^2 \psi}{\partial r \partial \theta}\right)g_9 + \left(\frac{1}{r^2}\frac{\partial w}{\partial \theta} - \frac{1}{r}\frac{\partial^2 w}{\partial r \partial \theta}\right)g_{10} \tag{20c}$$

where g_i $(i = 1, 2, \ldots, 10)$ are as follows:

$$\begin{aligned} &g_1 = B_{11}d_1 + B_{12}d_2,\quad g_2 = B_{11}d_2 + B_{12}d_5 \\ &g_3 = B_{11}d_3 + B_{12}d_7 + D_{11}, \\ &g_4 = B_{11}d_4 + B_{12}d_7 + D_{12} \\ &g_5 = B_{22}d_5 + B_{12}d_2,\quad g_6 = B_{22}d_2 + B_{12}d_1 \\ &g_7 = B_{22}d_6 + B_{12}d_4 + D_{22}, \\ &g_8 = B_{22}d_7 + B_{12}d_3 + D_{12} \\ &g_9 = B_{66}d_8,\quad g_{10} = B_{66}d_9 + D_{66} \end{aligned} \tag{21}$$

To derive the compatibility equation in terms of w and ψ, Eqs. (6), (17) and (18) are substituted into Eq. (7) in the following form:

$$\begin{aligned} &d_5\frac{\partial^4 \psi}{\partial r^4} + \frac{2}{r}d_5\frac{\partial^3 \psi}{\partial r^3} + \frac{1}{r^2}\left(\begin{matrix} d_2\frac{\partial^4 \psi}{\partial r^2 \partial \theta^2} - d_1\frac{\partial^2 \psi}{\partial r^2} \\ + d_8\frac{\partial^4 \psi}{\partial r^2 \partial \theta^2} + d_2\frac{\partial^4 \psi}{\partial r^2 \partial \theta^2} \end{matrix}\right) \\ &+ \frac{1}{r^3}\left(d_1\frac{\partial \psi}{\partial r} - d_8\frac{\partial^3 \psi}{\partial r \partial \theta^2} - 2d_2\frac{\partial^3 \psi}{\partial r \partial \theta^2}\right) \\ &+ \frac{1}{r^4}\left(d_8\frac{\partial^2 \psi}{\partial \theta^2} + d_1\frac{\partial^4 \psi}{\partial \theta^4} + 2d_2\frac{\partial^2 \psi}{\partial \theta^2} + 2d_1\frac{\partial^2 \psi}{\partial \theta^2}\right) \end{aligned} \tag{22}$$

$$
\begin{aligned}
&= d_7\frac{\partial^4 w}{\partial r^4} - \frac{1}{R}\left(\frac{\partial^2 w}{\partial r^2} + \frac{1}{r}\frac{\partial w}{\partial r} + \frac{1}{r^2}\frac{\partial^2 w}{\partial \theta^2}\right)\\
&+\frac{1}{r}\left(d_6\frac{\partial^3 w}{\partial r^3} - d_3\frac{\partial^3 w}{\partial r^3} - \frac{\partial w}{\partial r}\frac{\partial^2 w}{\partial r^2} + 2d_7\frac{\partial^3 w}{\partial r^3}\right)\\
&+\frac{1}{r^2}\left(\left(\frac{\partial^2 w}{\partial r\partial\theta}\right)^2 - \frac{\partial^2 w}{\partial r^2}\frac{\partial^2 w}{\partial \theta^2} - d_4\frac{\partial^2 w}{\partial r^2} + d_3\frac{\partial^4 w}{\partial r^2\partial\theta^2}\right.\\
&\qquad\left. + d_6\frac{\partial^4 w}{\partial r^2\partial\theta^2} - d_9\frac{\partial^4 w}{\partial r^2\partial\theta^2}\right)\\
&+\frac{1}{r^3}\left(d_4\frac{\partial w}{\partial r} + d_9\frac{\partial^3 w}{\partial r\partial\theta^2} - 2d_6\frac{\partial^3 w}{\partial r\partial\theta^2} - 2\frac{\partial w}{\partial\theta}\frac{\partial^2 w}{\partial r\partial\theta}\right)\\
&+\frac{1}{r^4}\left(\left(\frac{\partial w}{\partial\theta}\right)^2 - d_9\frac{\partial^2 w}{\partial\theta^2} + 2d_4\frac{\partial^2 w}{\partial\theta^2} - 2d_6\frac{\partial^2 w}{\partial\theta^2} + \frac{\partial^4 w}{\partial\theta^4}{b_4}^r\right)
\end{aligned}
$$

To derive the equation of motion in terms of w and ψ, Eqs. (5), (17) and (20) are substituted into Eq. (15) in the following form:

$$
\begin{aligned}
&Rr^2(g_1 + g_5 - 2g_9)\frac{\partial^4\psi}{\partial r^2\partial\theta^2}\\
&-Rr^2(g_4 + g_8 + 2g_{10})\frac{\partial^4 w}{\partial r^2\partial\theta^2} + Rg_6\frac{\partial^4\psi}{\partial\theta^4} - Rg_7\frac{\partial^4 w}{\partial\theta^4}\\
&+Rr^4 g_2\frac{\partial^4\psi}{\partial r^4} - Rr^4 g_3\frac{\partial^4 w}{\partial r^4} + Rr^3(g_1 - g_5 + 2g_2)\frac{\partial^3\psi}{\partial r^3}\\
&-Rr^3(2g_3 + g_4 - g_8)\frac{\partial^3 w}{\partial r^3} - 2Rr(g_1 - g_9)\frac{\partial^3\psi}{\partial r\partial\theta^2}\\
&+2Rr(g_4 + g_{10})\frac{\partial^3 w}{\partial r\partial\theta^2}\\
&+\left(Rr^2\frac{\partial^2 w}{\partial r^2} + R(2g_1 + 2g_6 - 2g_9) + r^2\right)\frac{\partial^2\psi}{\partial\theta^2}\\
&-r^2\left(-Rr\frac{\partial w}{\partial r} + Rg_6 - R\frac{\partial^2 w}{\partial\theta^2} - r^2\right)\frac{\partial^2\psi}{\partial r^2}\\
&-2R(+g_7 + g_4 + g_{10})\frac{\partial^2 w}{\partial\theta^2} + 2Rr\left(-r\frac{\partial^2 w}{\partial r\partial\theta} + \frac{\partial w}{\partial\theta}\right)\frac{\partial^2\psi}{\partial r\partial\theta}\\
&+Rr^2\left(r\frac{\partial\psi}{\partial r} + g_7\right)\frac{\partial^2 w}{\partial r^2} + 2Rr\frac{\partial\psi}{\partial\theta}\frac{\partial^2 w}{\partial r\partial\theta}\\
&-2R\frac{\partial w}{\partial\theta}\frac{\partial\psi}{\partial\theta} + (Rrg_6 + r^3)\frac{\partial\psi}{\partial r} - Rrg_7\frac{\partial w}{\partial r} - r^4 q\\
&= 2Rr^4\rho_1\mu\frac{\partial w}{\partial t} + Rr^4\rho_1\frac{\partial^2 w}{\partial t^2}
\end{aligned}
\tag{23}
$$

The compatibility equation (Eq. (22)) and equation of motion (Eq. (23)) are utilized to examine the vibration analysis and nonlinear dynamic stability of sandwich FG-CNTRC shallow spherical shells.

3.1 Boundary conditions

The sandwich FG-CNTRC shallow spherical shell is assumed to be clamped and immovable at its base edge ($r = r_0$), which is exposed to external pressure so that the loading is uniformly distributed on the outer surface of the shell, as shown in Fig. 5.

According to Fig. 5, the boundary conditions can be written as follows:

$$
\begin{aligned}
&u = 0, \qquad w = \frac{\partial w}{\partial r} = 0,\\
&N_r = N_0, \qquad N_{r\theta} = 0 \ \ at \ \ r = r_0
\end{aligned}
\tag{24}
$$

Also, boundary edge immovability conditions of the shallow spherical shell are fulfilled regarding the average sense as close conditions as follows:

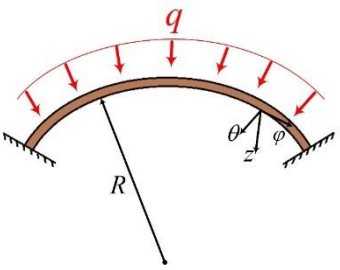

Fig. 5 Schematic of sandwich FG-CNTRC shallow spherical shell exposed to external pressure

$$
\int_0^{\pi}\int_0^{r_0}\frac{\partial u}{\partial r}r dr d\theta = 0 \tag{25}
$$

According to the boundary conditions (Eq. (24)), the approximate solution for the deflection (w) is represented by suitable mode functions, which consist of the three modes of transverse nonlinear oscillations. One function is chosen to represent the change in the symmetrically deformed shape of the shell (Tillman 1970), and the $n = 1$ and $n = 2$ asymmetrical mode functions are chosen to represent closely the shapes deduced by Huang (1964) that these functions are as follows:

$$
\begin{aligned}
w(r,\theta,t) = &\frac{W_1(-r^2 + r_0^2)^2}{r_0^4} + \frac{W_2 r(-r^2 + r_0^2)^2\cos(\theta)}{r_0^5}\\
&+\frac{W_3 r^2(-r^2 + r_0^2)^2\cos(2\theta)}{r_0^6}
\end{aligned}
\tag{26}
$$

where $W_1 = W_1(t)$, $W_2 = W_2(t)$, and $W_3 = W_3(t)$ are the three order modes of time-dependent unknown amplitudes, respectively. $\frac{(-r^2+r_0^2)^2}{r_0^4}$, $\frac{r(-r^2+r_0^2)^2\cos(\theta)}{r_0^5}$ and $\frac{r^2(-r^2+r_0^2)^2\cos(2\theta)}{r_0^6}$ are the three shape functions, respectively, which satisfy the boundary conditions. To obtain the stress function (ψ), Eq. (26) must be substituted in the compatibility equation (Eq. (22)), and then by solving the obtained PDE, the suitable stress function is extracted. But obtaining a suitable stress function via this method is difficult and complicated. Instead, it is more convenient to consider a stress function (ψ) similar to the approximate solution for the deflection. It should be noted that the selected stress function must be satisfied with the boundary conditions (Eq. (24)). Accordingly, the stress function can be chosen as follows:

$$
\begin{aligned}
\psi(r,\theta) = &\frac{F_1(-r^2 + r_0^2)^2}{r_0^4} + \frac{F_2 r(-r^2 + r_0^2)^2\cos(\theta)}{r_0^5}\\
&+\frac{F_3 r^2(-r^2 + r_0^2)^2\cos(2\theta)}{r_0^6} + \frac{1}{2}N_0 r^2
\end{aligned}
\tag{27}
$$

By substituting Eqs. (26) and (27) into Eq. (22), and applying the Galerkin method, a set of three equations in terms of F_i $(i = 1,2,3)$ are obtained as follows:

$$
\begin{aligned}
F_1 = &\frac{W_2^2}{10(d_1 - 9d_5)} + \frac{W_3^2}{35(d_1 - 9d_5)} + \frac{3W_1^2}{5(d_1 - 9d_5)}\\
&+\frac{(3d_3 - 3d_6 - 9d_7 + d_4)W_1}{(d_1 - 9d_5)} - \frac{W_1 r_0^2}{2R(d_1 - 9d_5)}
\end{aligned}
\tag{28a}
$$

$$F_2 = \frac{-2W_2W_3}{7(d_8+d_1+2d_2+9d_5)} + \frac{(d_3+d_4+d_6+9d_7+d_9+2r_0^2)W_2}{(d_8+d_1+2d_2+9d_5)} - \frac{4W_2W_1}{5(d_8+d_1+2d_2+9d_5)} \quad (28b)$$

$$F_3 = \frac{-5W_2^2}{7(8d_1+10d_2+30d_5+5d_8)} + \frac{(5d_3+8d_4+5d_6+30d_7-5d_9)W_3}{(8d_1+10d_2+30d_5+5d_8)} + \frac{W_3r_0^2}{R(8d_1+10d_2+30d_5+5d_8)} - \frac{8W_3W_1}{(56d_1+70d_2+210d_5+35d_8)} \quad (28c)$$

Substituting Eqs. (6), (17), (18) and (27) into Eq. (26), and by integrating, we can obtain N_0 in the following form:

$$N_0 = -2\frac{\begin{matrix}(A_{12}B_{12}-A_{12}B_{22}-A_{22}B_{11}+A_{22}B_{12})W_1\\+(A_{12}+A_{22})F_1\end{matrix}}{r_0^2(A_{12}-A_{22})} \quad (29)$$

Substituting F_1 of Eq. (28a) into Eq. (29), N_0 is calculated as:

$$N_0 = \frac{-2}{r_0^2(A_{12}-A_{22})}\left[\begin{pmatrix}A_{12}B_{12}-A_{12}B_{22}\\-A_{22}B_{11}+A_{22}B_{12}\end{pmatrix}W_1 + \frac{1}{R(70d_1-630d_5)}\left\{(A_{12}+A_{22})\begin{pmatrix}7RW_2^2+2RW_3^2\\+210d_3RW_1\end{pmatrix} +42RW_1^2+70d_4RW_1-210d_6RW_1-630d_7RW_1 \\ -35W_1r_0^2)\right\}\right] \quad (30)$$

Finally, by substituting Eqs. (26), (27), (28), and 30 into Eq. (23), and applying the Galerkin method, the nonlinear second-order ordinary differential equations for W_i $(i = 1,2,3)$, are obtained in the following form:

$$\begin{aligned}&\ddot{W}_1+2\mu\dot{W}_1+b_{11}W_1+b_{12}W_1^2+b_{13}W_1^3\\&+b_{14}W_1W_2^2+b_{15}W_1W_3^2+b_{16}W_3W_2^2\\&+b_{17}W_2^2+b_{18}W_3^2+b_{19}q=0\\&\ddot{W}_2+2\mu\dot{W}_2+b_{21}W_2+b_{22}W_2W_1^2\\&+b_{23}W_2W_1+b_{24}W_2W_3+b_{25}W_3W_1^2\\&+b_{26}W_2W_3^2+b_{27}W_1W_2W_3=0\\&\ddot{W}_3+2\mu\dot{W}_3+b_{31}W_3+b_{32}W_2^2+b_{33}W_3^3\\&+b_{34}W_3W_2^2+b_{35}W_1W_2^2+b_{36}W_3W_1^2\\&+b_{37}W_1W_3=0\end{aligned} \quad (31)$$

where the coefficients b_{ij} are too long to be explicitly presented here, they can be easily computed with computer algebra. Putting $W = W_{max}$, from Eq. (26), it is obvious that the maximum deflection of the sandwich FG-CNTRC shallow spherical shells:

$$W = W_1 + W_2 + W_3 \quad (32)$$

Eq. (31) is utilized to analyze the influences of input parameters on the load-maximum deflection curves of the sandwich FG-CNTRC shallow spherical shells.

3.2 Nonlinear vibration analysis

Considering the sandwich FG-CNTRC shallow spherical shells subjected to uniformly external pressure as $q = Q\sin\Omega t$, Eq. (31) can be written in the following form:

$$\begin{aligned}&\ddot{W}_1+2\mu\dot{W}_1+b_{11}W_1+b_{12}W_1^2+b_{13}W_1^3\\&+b_{14}W_1W_2^2+b_{15}W_1W_3^2+b_{16}W_3W_2^2\\&+b_{17}W_2^2+b_{18}W_3^2+b_{19}Q\,sin\,\Omega\,t=0\\&\ddot{W}_2+2\mu\dot{W}_2+b_{21}W_2+b_{22}W_2W_1^2\\&+b_{23}W_2W_1+b_{24}W_2W_3+b_{25}W_3W_1^2\\&+b_{26}W_2W_3^2+b_{27}W_1W_2W_3=0\\&\ddot{W}_3+2\mu\dot{W}_3+b_{31}W_3+b_{32}W_2^2+b_{33}W_3^3\\&+b_{34}W_3W_2^2+b_{35}W_1W_2^2+b_{36}W_3W_1^2\\&+b_{37}W_1W_3=0\end{aligned} \quad (33)$$

where Q is the amplitude of excitation and Ω is excitation frequency. The nonlinear vibration responses of the sandwich FG-CNTRC shallow spherical shells can be obtained by solving Eq. (3) by the fourth-order Runge-Kutta method.

To analyze the linear and free vibration of sandwich FG-CNTRC shallow spherical shells, the nonlinear terms and external load in Eq. (33) are neglected in the following form:

$$\begin{aligned}&\ddot{W}_1+b_{11}W_1=0\\&\ddot{W}_2+b_{21}W_2=0\\&\ddot{W}_3+b_{31}W_3=0\end{aligned} \quad (34)$$

According to Eq. (34), the natural frequency (ω_i $(i = 1,2,3)$) of the sandwich FG-CNTRC shallow spherical shells can be written in the following form:

$$\omega_1=\sqrt{b_{11}};\omega_2=\sqrt{b_{21}};\omega_3=\sqrt{b_{31}} \quad (35)$$

3.3 Dynamic post-buckling analysis

To analyze the dynamic post-buckling, in Eq. (31), the external load is varied as a linear function of time $q = ct$, in which $c(\mathrm{N/m^2s})$ is the speed of loading. By considering the external load in the mentioned form, the nonlinear relation for dynamic post-buckling of the sandwich FG-CNTRC shallow spherical shells is investigated in the following form:

$$\begin{aligned}&\ddot{W}_1+2\mu\dot{W}_1+b_{11}W_1+b_{12}W_1^2+b_{13}W_1^3\\&+b_{14}W_1W_2^2+b_{15}W_1W_3^2+b_{16}W_3W_2^2\\&+b_{17}W_2^2+b_{18}W_3^2+b_{19}ct=0\\&\ddot{W}_2+2\mu\dot{W}_2+b_{21}W_2+b_{22}W_2W_1^2\\&+b_{23}W_2W_1+b_{24}W_2W_3+b_{25}W_3W_1^2\\&+b_{26}W_2W_3^2+b_{27}W_1W_2W_3=0\\&\ddot{W}_3+2\mu\dot{W}_3+b_{31}W_3+b_{32}W_2^2\\&+b_{33}W_3^3+b_{34}W_3W_2^2+b_{35}W_1W_2^2\\&+b_{36}W_3W_1^2+b_{37}W_1W_3=0\end{aligned} \quad (36)$$

Because solving Eq. (36), using the analytical method is very hard and complicated, so, to solve this equation, the fourth-order Runge-Kutta method is utilized. Also, according to the Budiansky-Roth criterion (Budiansky 1962), the critical dynamic buckling loads are calculated. It should be explained that according to this criterion, the displacement response increases sharply depending on the time in the time-domain curve for large values of loading speed. Also, the maximum value of the curve is obtained by passing from a slope point. At the corresponding time $t = t_{cr}$,

Table 1 Comparison of the critical dynamic buckling of clamped FG shallow spherical shell with the change of index k ($P_{cr} \times 10^5$, $R/h = 1000$, $r_0/R = 0.2$, $\rho_c = 2370\ \mathrm{kg/m^3}$, $\rho_m = 8166\ \mathrm{kg/m^3}$, $E_c = 348.43\ \mathrm{GPa}$, $E_m = 201.04\ \mathrm{GPa}$, $\upsilon = 0.3$)

k	present	Duc *et al.* (2017)		Bich and Van Dung (2012)	
		4.1	Discrepancy (%)		Discrepancy (%)
0	2.9446	3.0135	2.28	2.9995	1.83
1	2.3469	2.4289	3.37	2.3796	1.37
5	1.9347	2.1254	8.97	1.9767	2.12
10	1.8425	1.9263	4.35	1.8826	2.13

Table 2 Comparison of the critical dynamic buckling of clamped FG shallow spherical shell with the change of index R/h ($P_{cr} \times 10^5$, $k = 1$, $r_0/R = 0.2$, $\rho_c = 2370\ \mathrm{kg/m^3}$, $\rho_m = 8166\ \mathrm{kg/m^3}$, $E_c = 348.43\ \mathrm{GPa}$, $E_m = 201.04\ \mathrm{GPa}$, $\upsilon = 0.3$)

R/h	present	Duc *et al.* (2017)		Bich and Van Dung (2012)	
		4.1	Discrepancy (%)		Discrepancy (%)
1000	2.3469	2.3812	1.44	2.3796	1.37
1200	1.9258	2.0039	3.89	1.9565	1.56
1500	1.5223	1.5108	0.76	1.5505	1.81
2000	1.1332	1.1327	0.04	1.1579	2.13

Table 3 Comparison of the natural frequencies of S-FGM shallow spherical shell (ω_1) with the change of volume fractions k ($P_{cr} \times 10^5$, $r_0/R = 0.2$, $R/h = 100$, $R = 3$, $\rho_c = 3800\ \mathrm{kg/m^3}$, $\rho_m = 2702\ \mathrm{kg/m^3}$, $E_c = 380\ \mathrm{GPa}$, $E_m = 70\ \mathrm{GPa}$, $\upsilon = 0.3$)

k	present	Duc *et al.* (2017)	
			Discrepancy (%)
0	5314.5	5314.2	2.28
1	10132.2	10132.6	3.37
5	12774.4	12774.0	8.97
∞	14057.4	14057.2	4.35

Table 4 The CNT/ matrix efficiency parameters

V^*_{CNT}	η_1	η_2	η_3
0.12	0.137	1.022	0.715

Table 5 The material properties of the CNTs

	ν_{12}^{CNT}	E_{11}^{CNT} (TPa)	E_{22}^{CNT} (TPa)	G_{12}^{CNT} (TPa)
$T = 300$ K	0.175	5.6466	7.0800	1.9445

which is called dynamic critical time, the stability loss occurs and the dynamic critical buckling load can be determined. It should be noted that unlike the static analysis which instability occurs in a definite point, in dynamic buckling analysis there is a region of instability where the

Table 6 The material properties of the composite matrix

ν^m	$\rho^m(\mathrm{kg/m^3})$	$E^m(\mathrm{GPa})$
0.34	1150	3.52

Table 7 The geometrical parameters of sandwich FG-CNTRC shallow spherical shell

R(m)	r_0(m)	h(m)	h_i $(i = 1,2,3)$
10	2	0.01	$h/3$

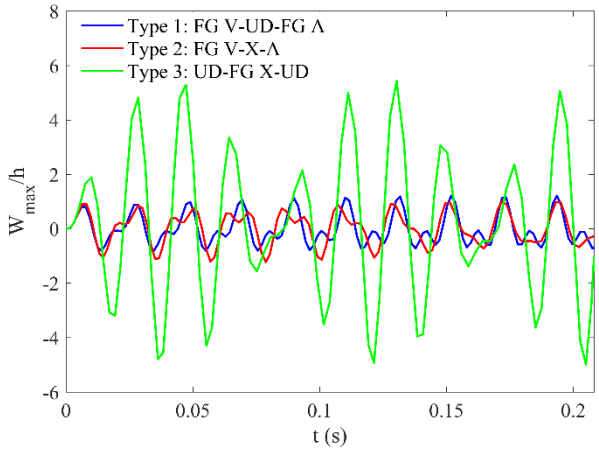

Fig. 6 nonlinear vibration responses of the sandwich FG-CNTRC shallow spherical shells for three types of layers of FG-CNTRC

4. Numerical results

4.1 Validation of this study

In this section, we first validate the suggested approach by available results in the literature. To this end, regarding the results presented by Duc *et al.* (2017) and Bich and Van Dung (2012), the FG shallow spherical shell is chosen. The boundary conditions are assumed as clamped at the edge, and the shell is assumed to be under uniform external pressure. The critical dynamic buckling response of the clamped FG shallow spherical shell with $n = 1$ asymmetrical mode functions for change of index k and R/h, respectively, is listed in Tables 1 and 2. The material properties are composed of silicon nitride (Si3N4) and steel (SUS 304). As a second validation, in Table 3, the natural frequencies of the S-FGM spherical shells are compared with the results obtained by Duc *et al.* (2017). As can be seen that there is a good agreement between these results. The mass density and Young's modulus of the FG shell are defined as:

$$\rho(z) = \rho_m + \frac{(\rho_c - \rho_m)}{k-1};\ E(z) = E_m + \frac{(E_c - E_m)}{k-1} \quad (37)$$

4.2 Material properties of the sandwich FG-CNTRC shallow spherical shells

In this sub-section, the nonlinear dynamic stability and vibration analysis of sandwich shallow spherical shells is

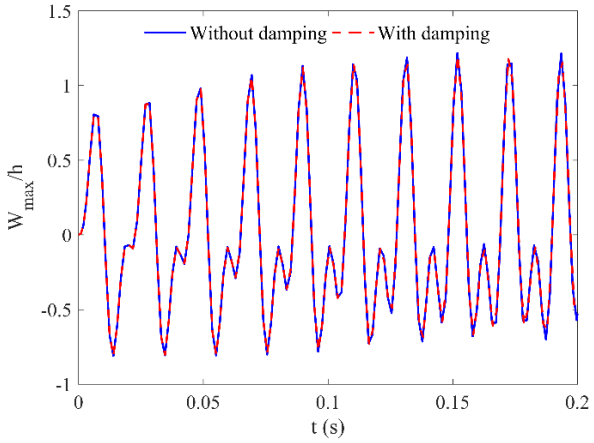

Type 1: FG V-UD-FG Λ

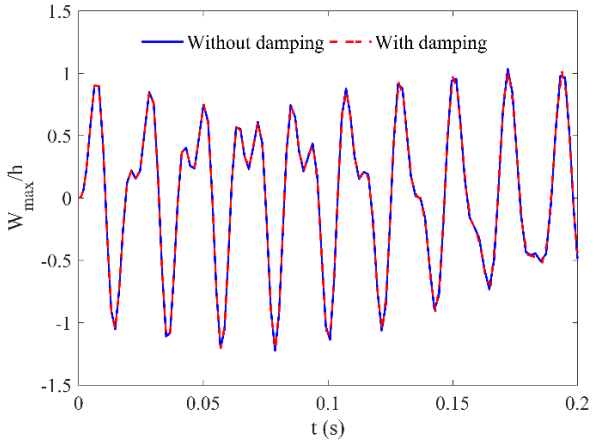

Type 2: FG V-X-Λ

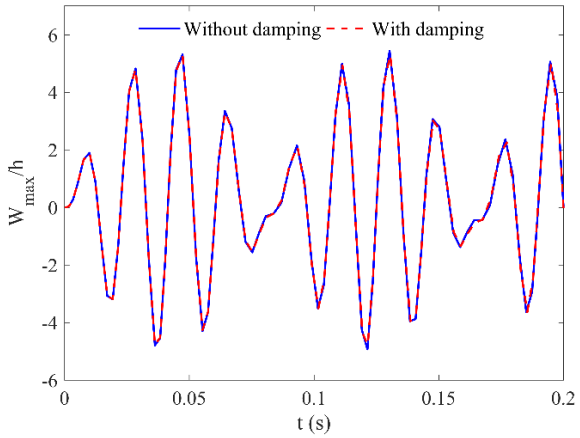

Type 3: UD-FG X-UD

Fig. 7 Influence of damping on the nonlinear vibration responses of the sandwich FG-CNTRC shallow spherical shells in the first periods

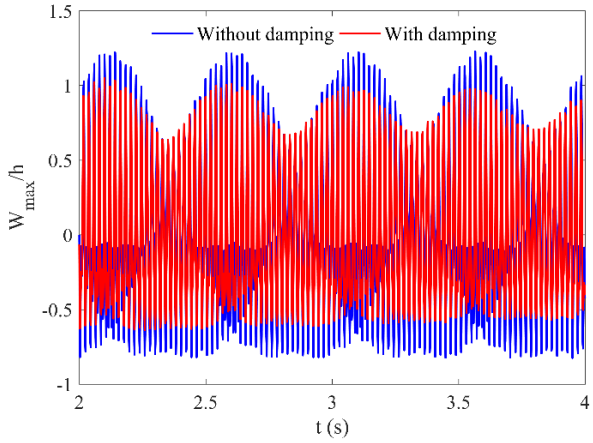

Type 1: FG V-UD-FG Λ

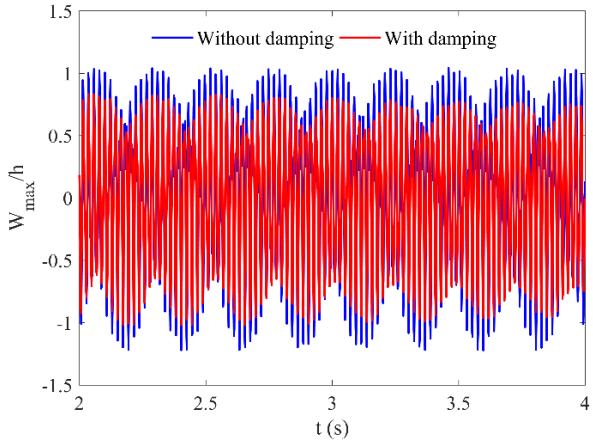

Type 2: FG V-X-Λ

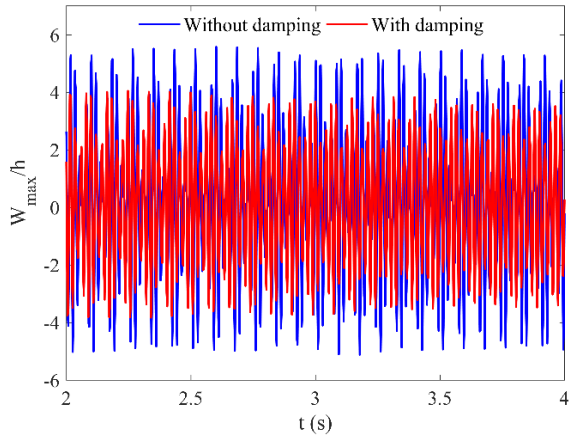

Type 3: UD-FG X-UD

Fig. 8 Influence of damping on the nonlinear vibration responses of the sandwich FG-CNTRC shallow spherical shells in the far periods

investigated. The effects of material parameters and various geometrical characteristics are presented. Poly (methyl methacrylate), referred to as PMMA, is selected as the matrix, and the (10,10) SWCNTs are selected as the reinforcement. In the present work, $V_{CNT}^{*} = 0.12$, and the parameters of the CNT/matrix efficiency are listed in Table4 (Choe *et al.* 2018, Wang and Pyrz 2004). Also, the material properties of the CNTs and composite matrix and the geometrical parameters of sandwich FG-CNTRC shallow spherical shell are presented in Tables 5-7, respectively.

4.3 Nonlinear vibration results

Fig. 6 illustrates the nonlinear vibration behaviors of the sandwich FG-CNTRC shallow spherical shells for three

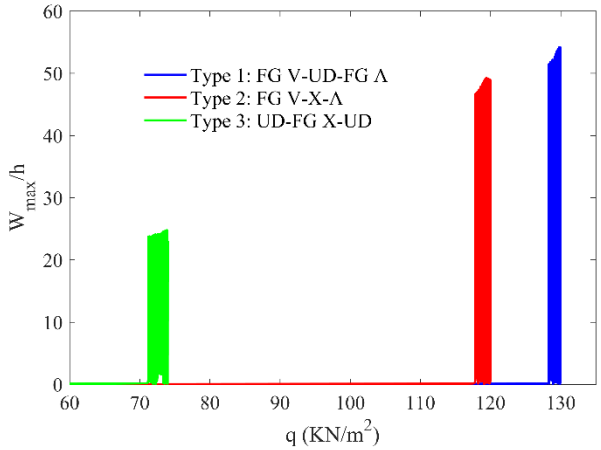

Fig. 9 Dynamic post-buckling responses of the sandwich FG-CNTRC shallow spherical shells for three types of layers of FG-CNTRC

different pattern types of FG-CNTRC. In order to the excitation frequencies are much smaller than natural frequencies, the external pressure is chosen as: $10^4\sin(300t)$. The vibration amplitude of the sandwich FG-CNTRC shallow spherical shells with type 3 and type 2 is maximum and minimum, respectively. In other words, if the order of the layers of the sandwich FG-CNTRC shallow spherical shells to be UD-FG X-UD, the vibration amplitude becomes maximum and if the order of the layers of the sandwich FG-CNTRC shallow spherical shells to be FG-V-X-Λ, the vibration amplitude becomes minimum. The reason is that the vibration amplitude strongly depends on the placement of the CNT in each layer. Also, according to the placing of the CNT in the UD-FG X-UD case and the FG-V-X-Λ case, the coefficients of strains in Eq. (8) and, consequently the strength of the system are respectively decreased and increased. So, decreasing and increasing the strength of the system, respectively, leads to increasing and decreasing the vibration amplitude.

The influence of damping on the nonlinear vibration responses of the sandwich FG-CNTRC shallow spherical shells for three pattern types is shown in Figs. 7 and 8 with linear damping coefficient $\mu = 0.3$ (Duc *et al.* 2017a). According to Fig. 7, the effect of damping is negligible to the nonlinear vibration response in the first vibration periods; however, as can be seen in Fig. 8, it strongly decreases amplitude at the next far periods. Considering that the system is nonlinear and exposed to external excitation, the linear damping in the first vibration periods could not completely reduce the vibration amplitude. So, it exponentially reduces the vibration amplitude at the next far periods.

4.4 Dynamic post-buckling results

The dynamic post-buckling response of the sandwich FG-CNTRC shallow spherical shells for three types of layers of FG-CNTRC is demonstrated in Fig. 9. The external

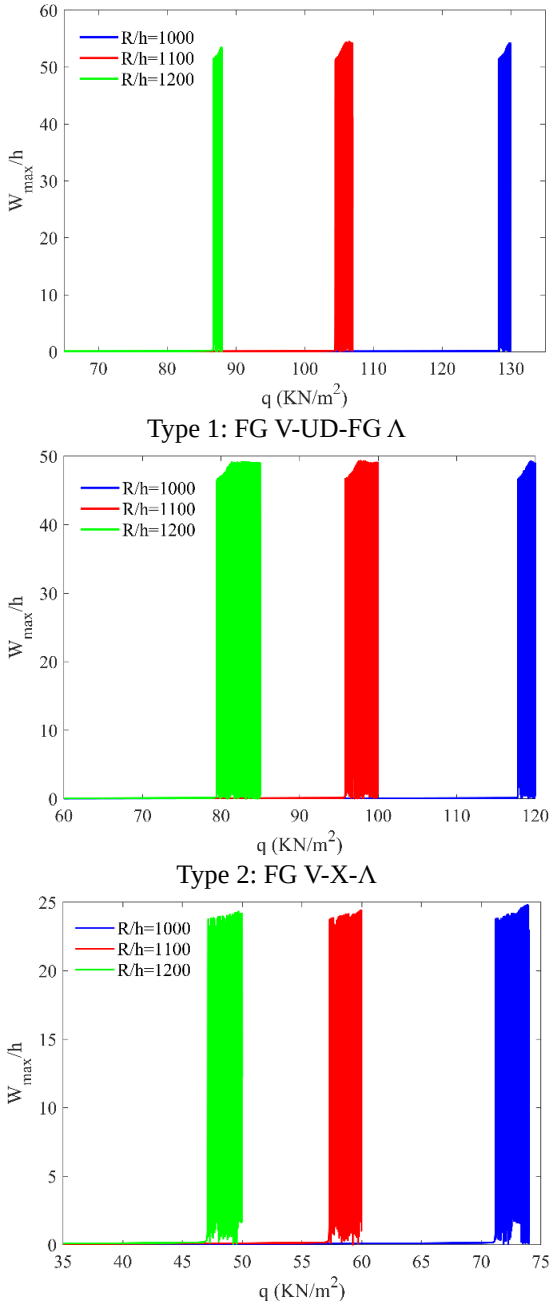

Fig. 10 Dynamic post-buckling behaviors of the sandwich FG-CNTRC shallow spherical shells for various radius versus thickness (R/h)

pressure is chosen as: $10^4 t$. The critical dynamic buckling of the sandwich FG-CNTRC shallow spherical shells with type 1 and type 3 is maximum and minimum, respectively. But, the minimum peak for the sandwich FG-CNTRC shallow spherical shells with type 1 and type 3 is less and more than others, respectively. In other words, if the order of the layers of the sandwich FG-CNTRC shallow spherical shells to be FG V-UD-FG Λ, the critical dynamic buckling becomes maximum, whereas, if the order of the layers of the sandwich FG-CNTRC shallow spherical shells to be UD-FG X-UD, the critical dynamic buckling becomes

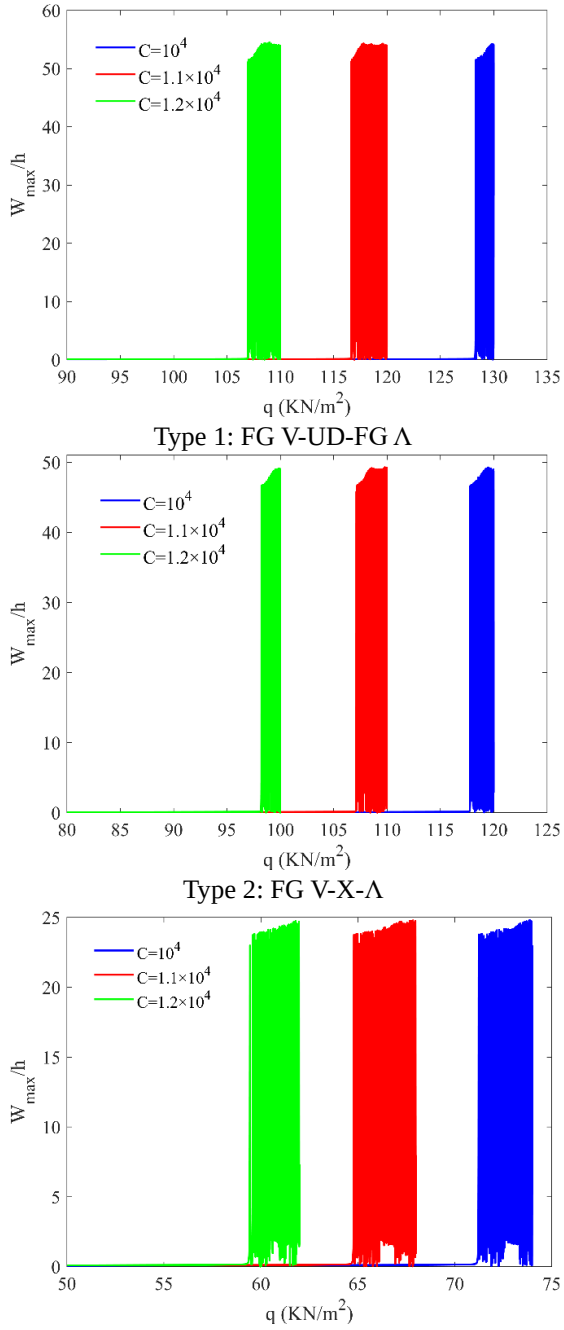

Type 1: FG V-UD-FG Λ

Type 2: FG V-X-Λ

Type 3: UD-FG X-UD

Fig. 11 The influences of the loading speed on the dynamic post-buckling responses of the sandwich FG-CNTRC shallow spherical shells

minimum. In this sub-section, similar to the previous sub-section, according to the placing of the CNT in the UD-FG X-UD case and the FG-V-X-Λ case, the resistance of the system and consequently, the dynamic buckling load-bearing capacity of the system are, respectively decreased and increased.

The dynamic post-buckling behaviors of the sandwich FG-CNTRC shallow spherical shells for various radius versus thickness (R/h) are illustrated in Fig. 10. The critical dynamic buckling of the sandwich FG-CNTRC shallow spherical shells is decreased by increasing the radius versus thickness.

The influences of the loading speed on the dynamic post-buckling responses of the sandwich FG-CNTRC shallow spherical shells are illustrated in Fig. 11. By increasing the loading speed, the critical dynamic buckling of the sandwich FG-CNTRC shallow spherical shells is decreased. Because by increasing the loading speed, the dynamic buckling load-bearing capacity of the sandwich FG-CNTRC shallow spherical shells is decreased, and consequently, the resistance against the dynamic buckling load is reduced.

5. Conclusions

A semi-analytical method was utilized to study the nonlinear dynamic stability and vibration analysis of sandwich shallow spherical shells. The sandwich shell is considered FG-CNTRC. The sandwich shallow spherical shells have three new patterns of FG-CNTRC. According to the von Kármán-Donnell nonlinear strain-displacement relations, and applying the Galerkin method, the nonlinear vibration problem has been solved. The Nonlinear dynamic stability is analyzed via the fourth-order Runge-Kutta method, and then the Budiansky-Roth criterion is employed to obtain the critical load for the dynamic post-buckling. The influences of various geometrical characteristics and material parameters on the nonlinear dynamic stability and vibration analysis of sandwich FG-CNTRC shallow spherical shells are investigated. Some of the main conclusions may be summarized as follows:

• If the order of the layers of the sandwich FG-CNTRC shallow spherical shells to be UD-FG X-UD, the vibration amplitude becomes maximum, and if the order of the layers of the sandwich FG-CNTRC shallow spherical shells to be FG V-X-Λ, the vibration amplitude becomes minimum.

• If the order of the layers of the sandwich FG-CNTRC shallow spherical shells to be FG V-UD-FG Λ, the critical dynamic buckling becomes maximum, whereas, if the order of the layers of the sandwich FG-CNTRC shallow spherical shells to be UD-FG X-UD, the critical dynamic buckling becomes minimum.

• The effect of damping is very small to the nonlinear vibration response in the first vibration periods; however, it strongly decreases amplitude at the next far periods.

• By increasing the radius versus thickness, the critical dynamic buckling of the sandwich FG-CNTRC shallow spherical shells is decreased.

• By increasing the loading speed, the critical dynamic buckling of the sandwich FG-CNTRC shallow spherical shells is decreased.

References

Anh, V.T.T., Bich, D.H. and Duc, N.D. (2015), "Nonlinear stability analysis of thin FGM annular spherical shells on elastic foundations under external pressure and thermal loads", *Eur. J.*

Mech. A Solid., **50**, 28-38. https://doi.org/10.1016/j.euromechsol.2014.10.004.

Asadi, H. and Wang, Q. (2017), "Dynamic stability analysis of a pressurized FG-CNTRC cylindrical shell interacting with supersonic airflow", *Compos. B. Eng.*, **118**, 15-25. https://doi.org/10.1016/j.compositesb.2017.03.001.

Aydogdu, M. (2014), "On the vibration of aligned carbon nanotube reinforced composite beams", *Adv. Nano Res.*, **2**(4), 199-210. http://dx.doi.org/10.12989/anr.2014.2.4.199.

Bich, D.H. and Van Tung, H. (2011), "Non-linear axisymmetric response of functionally graded shallow spherical shells under uniform external pressure including temperature effects", *Int. J. Nonlin. Mech.*, **46**(9), 1195-1204. https://doi.org/10.1016/j.ijnonlinmec.2011.05.015.

Bich, D.H. and Van Dung, D. (2012), "Nonlinear static and dynamic buckling analysis of functionally graded shallow spherical shells including temperature effects", *Compos. Struct.*, **94**(9), 2952-2960. https://doi.org/10.1016/j.compstruct.2012.04.012.

Budiansky, B. (1962), "Axisymmetric dynamic buckling of clamped shallow spherical shells", *NASA TN 1510*, 597-606.

Chan D.Q., Nguyen P.D., Quang V.D., Anh V.T.T., Duc N.D. (2019), "Nonlinear buckling and post-buckling of functionally graded CNTs reinforced composite truncated conical shells subjected to axial load", *Steel Compos. Struct.*, **31**(3) 243-259. https://doi.org/10.12989/scs.2019.31.3.243.

Choe, K., Wang, Q. and Tang, J. (2018), "Vibration analysis for coupled composite laminated axis-symmetric doubly-curved revolution shell structures by unified Jacobi-Ritz method", *Compos. Struct.*, **194**, 136-157. https://doi.org/10.1016/j.compstruct.2018.03.095.

Cong, P.H., Trung, V.D., Khoa, N.D. and Duc, N.D. (2022), "Vibration and nonlinear dynamic response of temperature-dependent FG-CNTRC laminated double curved shallow shell with positive and negative Poisson's ratio", *Thin Wall. Struct.*, **171**, 108713. https://doi.org/10.1016/j.tws.2021.108713.

Dat, N.D., Khoa, N.D., Nguyen, P.D. and Duc, N.D. (2020), "An analytical solution for nonlinear dynamic response and vibration of FG-CNT reinforced nanocomposite elliptical cylindrical shells resting on elastic foundations", *J. Appl. Math. Mech.*, **100**(1), e201800238. https://doi.org/10.1002/zamm.201800238.

Dat, N.D., Thanh, N.V., MinhAnh, V. and Duc, N.D. (2022), "Vibration and nonlinear dynamic analysis of sandwich FG-CNTRC plate with porous core layer", *Mech. Adv. Mater. Struct.*, **29**(10), 1431-1448. https://doi.org/10.1080/15376494.2020.1822476.

Duc, N.D., Cong, P.H., Tuan, N.D., Tran, P. and Van Thanh, N. (2017b), "Thermal and mechanical stability of functionally graded carbon nanotubes (FG CNT)-reinforced composite truncated conical shells surrounded by the elastic foundations", *Thin Wall. Struct.*, **115**, 300-310. https://doi.org/10.1016/j.tws.2017.02.016.

Duc, N.D., Dao, H.B. and Vu, T.T.A. (2016), "On the nonlinear stability of eccentrically stiffened functionally graded annular spherical segment shells", *Thin Wall. Struct.*, **106**, 258-267. https://doi.org/10.1016/j.tws.2016.05.006.

Duc, N.D., Hadavinia, H., Quan, T.Q. and Khoa, N.D. (2019), "Free vibration and nonlinear dynamic response of imperfect nanocomposite FG-CNTRC double curved shallow shells in thermal environment", *Eur. J. Mech. A Solid.*, **75**, 355-366. https://doi.org/10.1016/j.euromechsol.2019.01.024.

Duc, N.D. (2013), "Nonlinear dynamic response of imperfect eccentrically stiffened FGM double curved shallow shells on elastic foundation", *Compos. Struct.*, **99**, 88-96. https://doi.org/10.1016/j.compstruct.2012.11.017.

Duc, N.D. (2014), "*Nonlinear Static And Dynamic Stability Of Functionally Graded Plates And Shells*", Vietnam Natl Univ Press, Hanoi, Vietnam.

Duc, N.D. (2018), "Nonlinear thermo-electro-mechanical dynamic response of shear deformable piezoelectric sigmoid functionally graded sandwich circular cylindrical shells on elastic foundations", *J. Sandw. Struct. Mater.*, **20**(3), 351-378. https://doi.org/10.1177/1099636216653266.

Duc, N.D., Quang, V.D. and Anh, V.T.T. (2017a), "The nonlinear dynamic and vibration of the S-FGM shallow spherical shells resting on an elastic foundations including temperature effects", *Int. J. Mech. Sci.*, **123**, 54-63. https://doi.org/10.1016/j.ijmecsci.2017.01.043.

Ebrahimi, F. and Habibi, S. (2017), "Low-velocity impact response of laminated FG-CNT reinforced composite plates in thermal environment", *Adv. Nano Res.*, **5**(2), 69-97. http://doi.org/10.12989/anr.2017.5.2.069.

Foroutan, K., Ahmadi, H. and Carrera, E. (2019), "Nonlinear vibration of imperfect FG-CNTRC cylindrical panels under external pressure in the thermal environment", *Compos. Struct.*, **227**, 111310. https://doi.org/10.1016/j.compstruct.2019.111310.

Foroutan, K., Carrera, E. and Ahmadi, H. (2021b), "Nonlinear hygrothermal vibration and buckling analysis of imperfect FG-CNTRC cylindrical panels embedded in viscoelastic foundations", *Eur. J. Mech. A-Solid.*, **85**, 104107. https://doi.org/10.1016/j.euromechsol.2020.104107.

Foroutan, K., Carrera, E. and Ahmadi, H. (2021a), "Static and dynamic hygrothermal postbuckling analysis of sandwich cylindrical panels with an FG-CNTRC core surrounded by nonlinear viscoelastic foundations", *Compos. Struct.*, **259**, 113214. https://doi.org/10.1016/j.compstruct.2020.113214.

Fu, T., Wu, X., Xiao, Z. and Chen, Z. (2021), "Dynamic instability analysis of FG-CNTRC laminated conical shells surrounded by elastic foundations within FSDT", *Eur. J. Mech. A Solids*, **85**, 104139. https://doi.org/10.1016/j.euromechsol.2020.104139.

Ganapathi, M. and Varadan, T. (1995), "Dynamic buckling of laminated anisotropic spherical caps", *J. Appl. Mech.*, **62**(1), 13-19. https://doi.org/10.1115/1.2895879.

Ganapathi, M. and Varadan, T. (1982), "Dynamic buckling of orthotropic shallow spherical shells", *Comput. Struct.*, **15**(5), 517-520. https://doi.org/10.1016/0045-7949(82)90003-7.

Hashemi, R., Mirzaei, M. and Adlparvar, M.R. (2021), "On thermally induced instability of FG-CNTRC cylindrical panels", *Adv. Nano Res.*, **10**(1), 43-57. http://doi.org/10.12989/anr.2021.10.1.043.

Huang, H. and Han, Q. (2010), "Nonlinear dynamic buckling of functionally graded cylindrical shells subjected to time-dependent axial load", *Compos. Struct.*, **92**(2), 593-598. https://doi.org/10.1016/j.compstruct.2009.09.011.

Huang, N.C. (1964), "Unsymmetrical buckling of thin shallow spherical shells", *J. Appl. Mech.*, **31**(3), 447-457. https://doi.org/10.1115/1.3629662.

Jamali, M., Shojaee, T., Mohammadi, B. and Kolahchi, R. (2019), "Cut out effect on nonlinear post-buckling behavior of FG-CNTRC micro plate subjected to magnetic field via FSDT", *Adv. Nano Res.*, **7**(6), 405-417. http://doi.org/10.12989/anr.2019.7.6.405.

Jiao, P., Chen, Z., Li, Y., Ma, H. and Wu, J. (2019), "Dynamic buckling analyses of functionally graded carbon nanotubes reinforced composite (FG-CNTRC) cylindrical shell under axial power-law time-varying displacement load", *Compos. Struct.*, **220**, 784-797. https://doi.org/10.1016/j.compstruct.2019.04.048.

Khadimallah, M.A., Hussain, M., Taj, M., Ayed, H. and Tounsi, A. (2021), "Parametric vibration analysis of single-walled carbon nanotubes based on Sanders shell theory", *Adv. Nano Res.*, **10**(2), 165-174. http://doi.org/10.12989/anr.2021.10.2.165.

Lei, Z., Zhang, L. and Liew, K.M. (2015), "Free vibration analysis of laminated FG-CNT reinforced composite rectangular plates

using the kp-Ritz method", *Compos. Struct.*, **127**, 245-259. https://doi.org/10.1016/j.compstruct.2015.03.019.

Loy, C., Lam, K. and Reddy, J. (1999), "Vibration of functionally graded cylindrical shells", *Int. J. Mech. Sci.*, **41**(3), 309-324. https://doi.org/10.1016/S0020-7403(98)00054-X.

Manh, D.T., Anh, V.T.T., Nguyen, P.D. and Duc, N.D. (2020), "Nonlinear post-buckling of CNTs reinforced sandwich-structured composite annular spherical shells", *Int. J. Struct. Stabil.*, **20**(2), 2050018. https://doi.org/10.1142/S0219455420500182.

Pan, B. and Cui W. (2011), "A comparison of different rules for the spherical pressure hull of deep manned submersibles", *Chuan Bo Li Xue J. Sh. Mech.*, **15**(3), 276-285. https://doi.org/10.1109/UT.2011.5774084.

Pan, B. and Cui, W. (2010), "An overview of buckling and ultimate strength of spherical pressure hull under external pressure", *Marine Struct.*, **23**(3), 227-240. https://doi.org/10.1016/j.marstruc.2010.07.005.

Phung-Van, P., Thanh, C.L., Nguyen-Xuan, H. and Abdel-Wahab, M. (2018), "Nonlinear transient isogeometric analysis of FG-CNTRC nanoplates in thermal environments", *Compos. Struct.*, **201**, 882-892. https://doi.org/10.1016/j.compstruct.2018.06.087.

Prakash, T., Sundararajan, N. and Ganapathi, M. (2007), "On the nonlinear axisymmetric dynamic buckling behavior of clamped functionally graded spherical caps", *J. Sound Vib.*, **299**(1-2), 36-43. https://doi.org/10.1016/j.jsv.2006.06.060.

Quan, T.Q. and Duc, N.D. (2016), "Nonlinear vibration and dynamic response of shear deformable imperfect functionally graded double-curved shallow shells resting on elastic foundations in thermal environments", *J. Therm. Stresses*, **39**(4), 437-459. https://doi.org/10.1080/01495739.2016.1158601.

Sankar, A., Natarajan, S., Merzouki, T. and Ganapathi, M. (2017), "Nonlinear dynamic thermal buckling of sandwich spherical and conical shells with CNT reinforced facesheets", *Int. J. Struct. Stab. Dyn.*, **17**(9), 1750100. https://doi.org/10.1142/S0219455417501000.

Seidel, G.D. and Lagoudas, D.C. (2006), "Micromechanical analysis of the effective elastic properties of carbon nanotube reinforced composites", *Mech. Mater.*, **38**(8-10), 884-907. https://doi.org/10.1016/j.mechmat.2005.06.029.

Shahsiah, R., Eslami, M. and Boroujerdy, M.S. (2011), "Thermal instability of functionally graded deep spherical shell", *Arch. Appl. Mech.*, **81**(10), 1455-1471. https://doi.org/10.1007/s00419-010-0495-7.

Shen, H.S. and Zhang, C.L. (2010), "Thermal buckling and postbuckling behavior of functionally graded carbon nanotube-reinforced composite plates", *Mater. Design*, **31**(7), 3403-3411. https://doi.org/10.1016/j.matdes.2010.01.048.

Shen, H.S. and Zhu, Z.H. (2010), "Buckling and postbuckling behavior of functionally graded nanotube-reinforced composite plates in thermal environments", *Comput. Mater. Continua*, **18**(2), 155-182. https://doi.org/10.3970/cmc.2010.018.155.

Tayeb, T.S., Zidour, M., Bensattalah, T., Heireche, H., Benahmed, A. and Bedia, E.A. (2020), "Mechanical buckling of FG-CNTs reinforced composite plate with parabolic distribution using Hamilton's energy principle", *Adv. Nano Res.*, **8**(2), 135-148. http://doi.org/10.12989/anr.2020.8.2.135.

Thai, C.H., Ferreira, A.J.M., Rabczuk, T. and Nguyen-Xuan, H. (2018), "Size-dependent analysis of FG-CNTRC microplates based on modified strain gradient elasticity theory", *Eur. J. Mech. A Solid.*, **72**, 521-538. https://doi.org/10.1016/j.euromechsol.2018.07.012.

Thanh, N.V., Khoa, N.D., Tuan, N.D., Tran, P. and Duc, N.D. (2017), "Nonlinear dynamic response and vibration of functionally graded carbon nanotube-reinforced composite (FG-CNTRC) shear deformable plates with temperature-dependent material properties and surrounded on elastic foundations", *J. Therm. Stresses*, **40**(10), 1254-1274. https://doi.org/10.1080/01495739.2017.1338928.

Thomas, B., Roy, T. (2016), "Vibration analysis of functionally graded carbon nanotube-reinforced composite shell structures", *Acta Mech.*, **227**(2), 581-599. https://doi.org/10.1007/s00707-015-1479-z.

Tillman, S. (1970), "On the buckling behaviour of shallow spherical caps under a uniform pressure load", *Int. J. Solid Struct.*, **6**(1), 37-52. https://doi.org/10.1016/0020-7683(70)90080-6.

Tounsi, A., Benguediab, S., Semmah, A. and Zidour, M. (2013), "Nonlocal effects on thermal buckling properties of double-walled carbon nanotubes", *Adv. Nano Res.*, **1**(1), 1-11. http://doi.org/10.12989/anr.2013.1.1.001.

Wang, A., Chen, H., Hao, Y., Zhang, W. (2018), "Vibration and bending behavior of functionally graded nanocomposite doubly-curved shallow shells reinforced by graphene nanoplatelets", *Results Phys.*, **9**, 550-559. https://doi.org/10.1016/j.rinp.2018.02.062.

Wang, X., Bradford, P.D., Liu, W., Zhao, H., Inoue, Y., Maria, J.P., Li, Q., Yuan, F.G. and Zhu, Y. (2011), "Mechanical and electrical property improvement in CNT/Nylon composites through drawing and stretching", *Compos. Sci. Technol.*, **71**(14), 1677-1683. https://doi.org/10.1016/j.compscitech.2011.07.023.

Wang, J. and Pyrz, R. (2004), "Prediction of the overall moduli of layered silicate-reinforced nanocomposites—part I: basic theory and formulas", *Compos. Sci. Technol.*, **64**(7-8), 925-934. https://doi.org/10.1016/S0266-3538(03)00024-1.

Wang, J., Li, Z.L. and Yu, W. (2019), "Structural similitude for the geometric nonlinear buckling of stiffened orthotropic shallow spherical shells by energy approach", *Thin Wall. Struct.*, **138**, 430-457. https://doi.org/10.1016/j.tws.2018.02.006.

Wang, Q., Cui, X., Qin, B. and Liang, Q. (2017), "Vibration analysis of the functionally graded carbon nanotube reinforced composite shallow shells with arbitrary boundary conditions", *Compos. Struct.*, **182**, 364-379. https://doi.org/10.1016/j.compstruct.2017.09.043.

Wunderlich, W. and Albertin, U. (2002), "Buckling behaviour of imperfect spherical shells", *Int. J. Nonlin. Mech.*, **37**(4-5), 589-604. https://doi.org/10.1016/S0020-7462(01)00086-5.

Ye, Z. (1997), "The non-linear vibration and dynamic instability of thin shallow shells", *J. Sound Vib.*, **202**(3), 303-311. https://doi.org/10.1006/jsvi.1996.0827.

Zhu, P., Lei, Z. and Liew, K.M. (2012), "Static and free vibration analyses of carbon nanotube-reinforced composite plates using finite element method with first order shear deformation plate theory", *Compos. Struct.*, **94**(4), 1450-1460. https://doi.org/10.1016/j.compstruct.2011.11.010.

CC